J Mol Model (2001) 7:207–215
DOI 10.1007/s008940100037

ORIGINAL PAPER

Xilin Yin · Huanmei Han · Akira Miyamoto

Structure and adsorption properties of MoO_3: insights from periodic density functional calculations

Received: 16 January 2001 / Accepted: 21 May 2001 / Published online: 10 July 2001

Abstract Structure and electronic properties of MoO_3 bulk and the (010) surface, as well as molecular adsorption of water on the (010) surface are investigated using periodic boundary density functional calculations. The bulk structure is calculated to be in good agreement with experiment. The structure and electronic properties of the (010) surface are confirmed to be very similar to those of the bulk. The terminal oxygen in both the bulk and the (010) surface is the least ionic among the three types of lattice oxygens. This study shows that the molecular adsorption of H_2O hardly takes place at the asymmetric and symmetric oxygens, but occurs at the terminal oxygen of the (010) surface. The results of the H_2O adsorption on the (010) at 1 and 0.5 monolayer coverages are interpreted based on charge-transfer interactions between the surface and H_2O species, and provide key information about the structural and energetic properties, in which each stable adsorption structure is suggested to orient on the surface via hydrogen bonding. These results also provide novel model systems for understanding the structure and adsorption states of MoO_3.

Keywords MoO_3 bulk · MoO_3 surface · Molybdenum trioxide · Adsorption · Density functional calculations

Introduction

Molybdenum trioxide (α-MoO_3) is one of the most important active compounds in catalysts for partial oxidation of hydrocarbons and for selective catalytic reduction (SCR) of NO_x by NH_3. In general, its lattice oxygens take part in the reactions, and the catalytic activity of MoO_3 depends mainly on the activity of the lattice oxygens. [1, 2] It is well known that three kinds of structurally different lattice oxygens in MoO_3 exist, i.e., terminal oxygen (singly coordinated, O_1), asymmetric bridging oxygen (doubly coordinated, O_2), and symmetric bridging oxygen (triply coordinated, O_3). Therefore, it is crucial to understand the chemical nature of the distinct oxygen species in order to clarify the activity of MoO_3. Much like V_2O_5, MoO_3 has an orthorhombic layered structure, with each layer comprising two interleaved planes of MoO_6 octahedra. The layers are parallel to the (010) crystal plane, and therefore the (010) plane is the most exposed and the thermodynamically most stable, where only O ions are exposed on the surface. [3]

So far, many experimental studies with respect to the structural and reactive properties of MoO_3 have been carried out, but the number of surface lattice oxygens that are active sites in the course of the catalysis has rarely been determined. [1, 2, 4] On the other hand, in contrast to the numerous experimental studies, theoretical investigations on this subject are relatively few. The structure and electronic properties of the MoO_3 bulk were investigated by means of ab initio Hartree–Fock (HF) techniques. [5, 6] It was reported that the nature of the Mo–O interaction changed considerably with the equilibrium bond distance, and varied from strongly covalent for the shortest bond to a predominantly ionic interaction for the longest bonds in the MoO_6 octahedron, and a weak attractive Coulombic force was active between adjacent layers. Molecular adsorption of H_2O on the (100) surface was studied by the ab initio HF method. It was found that H_2O molecularly adsorbed on the fivefold Mo atom (Lewis acid) of the surface mainly by electrostatic interaction. [5] However, adsorption on the surface lattice oxygens (Lewis base) has not been examined.

Hermann and coworkers [7, 8, 9, 10] investigated electronic properties of the clean (100) and (010) surfaces, and adsorption of H atom on the (010) and C_3H_5 (allyl) on the (100) and (010) surfaces using ab initio densi-

X. Yin (✉) · H. Han · A. Miyamoto
Department of Materials Chemistry,
Graduate School of Engineering, Tohoku University,
Aoba-yama 07, Aoba-ku, Sendai 980-8579, Japan
e-mail: yin@physics.queensu.ca
Tel.: +1-613-533 2723, Fax: +1-613-533 6463

X. Yin
Department of Physics, Queen's University,
Kingston, Ontario, Canada K7L 3N6

ty functional theory (DFT) calculations with a cluster approach. They observed that the terminal oxygen experienced the smallest negative charge, the asymmetric bridging oxygen was more negative, and the symmetric bridging oxygen became most negative. H adsorbed at all oxygen sites, but binding was strongest at the terminal site of the (010). The results of allyl adsorption on the (010) and (100) surfaces suggested that a starting point in the allyl to acrolein oxidation process should be on the (010) but not on the (100) surface. On the (010) surface, the allyl bound most strongly above an asymmetric bridging oxygen site with the adsorbate plane perpendicular to the surface. Chen et al. [11, 12] studied the clean and H-covered (010) surface and methyl reaction on the (010) using DFT pseudopotential calculations. They reported that the terminal oxygen exhibited covalent bonding to Mo that was stronger than each of the two bridging oxygens, and H was most strongly adsorbed over the terminal oxygen. When the coverage of CH_3 was 0.5 monolayer, methoxy was formed over the bridging oxygens; while the coverage reached 1, CH_3 was not stable and decomposed.

Using a semiempirical ASED-MO technique based on the traditional extended Hückel theory, Irigoyen et al. [13] studied the methane oxidation reaction on the (100) surface, where different sequences and sites for H-abstraction from methane were explored on layers exposing Mo or O atoms. They found that the process appeared to be endothermic and formation of oxygenated products was also addressed. They also studied the homolytic and heterolytic mechanisms of the CH_3- and CH_2-oxidation reactions on the (100) surface. [14] In addition, first principles calculations at HF, MP2 and B3LYP were performed to investigate electronic structure of molybdenum oxide clusters. [15]

It has been known for many years that the interaction of water molecules with metal oxide surfaces has important consequences for their catalytic behaviors, [16] since usually catalysts are exposed under the ambient conditions, and water exists in both reactants and products. In particular, water is always formed in selective oxidation reactions, and the role of the H_2O in these reactions has not yet been well investigated. [2] Moreover, it has not been well clarified which lattice oxygens of MoO_3 act as the active site in catalytic reactions. [1, 2, 4, 17] To the best of our knowledge, very few studies of H_2O adsorption on the catalytically important MoO_3(010) surface have been carried out so far. Towards a better understanding with respect to these issues, we have performed periodic first principles DFT calculations to investigate the structure and electronic properties of both MoO_3 bulk and the (010) surface, followed by investigating the adsorption properties of H_2O molecule on the (010) surface.

Methods

The periodic DFT calculations were performed using the CASTEP [18] and DSolid [19] codes. Our earlier studies of V_2O_5 bulk and the clean (010) surface, and adsorption of H atom and small molecules on the V_2O_5(010) surface [20, 21, 22, 23, 24] have shown that these methodologies are feasible and reliable, and they get rid of the restriction of the cluster approach.

The geometries of MoO_3 bulk and (010) surface, as well as H_2O adsorption systems are optimized by CASTEP, [18] which uses a conjugated gradient technique in a direct minimization of the Kohn–Sham energy functional and employs pseudopotentials to represent core electrons. The basis set used consisted of plane wave functions. In this approach Hellmann–Feynman forces on ions can be evaluated easily, and therefore geometry optimization can be performed to get stable structures. Exchange and correlation effects are included within the generalized gradient approximation (GGA) of Perdew and Wang. Gradient-corrected energies are computed self-consistently. A plane wave cutoff energy of 560 eV is used for which molybdenum and oxygen pseudopotentials are well converged. For hydrogen, its pure potential is used.

DSolid [19] within the Kohn–Sham formalism, [25] was used to perform Mulliken population analysis. A non-local type functional of PGX/P91 (Perdew 1991 exchange with Perdew 1991 correlation [26]) was employed. Molecular orbitals are expanded into a set of numerical atomic orbitals by double-numerical basis functions together with polarization functions (DNP). The DNP is comparable in quality to Pople's split-valence 6-31G** basis set and usually yields the most reliable results. [27, 28, 29] To reduce the necessary CPU time, the core orbitals of Mo and O atoms were frozen.

Our approach is as follows: CASTEP is used to optimize the geometries of MoO_3 bulk and (010) surface, as well as water adsorption systems at the GGA level, and then electronic structure calculations with respect to the equilibrium geometries obtained by CASTEP are performed using DSolid at the GGA. The adsorption energy (E_{ads}) is calculated according to the expression

$$E_{ads}=E_{adsorbate/substrate}-(E_{adsorbate}+E_{substrate})$$

where $E_{adsorbate/substrate}$ represents the total energy of the adsorbate/substrate system, $E_{adsorbate}$ and $E_{substrate}$ are the total energies of the isolated adsorbate and clean substrate, respectively. A negative adsorption energy corresponds to a stable adsorption system.

All models used in the current study have periodic boundaries. A unit cell consisting of four MoO_3 units was used to model the bulk structure. Since experimental investigation has revealed that catalytic reactions, for example the allyl to acrolein conversion, take place on MoO_3(010) but not on the (100) surfaces, [30] our studies to understand catalysis on MoO_3 have concentrated on the (010) surface. [3] Therefore, the MoO_3(010) surface was chosen to study the adsorption properties, which are strongly related to the catalytic properties. In

addition, owing to the rather weak interaction between layers in MoO_3, the weak Mo···O bond is easily broken to form the (010) surface, and hence the (010) is the most stable and similar to the bulk structure. [3] Therefore, the (010) surface was modeled by a periodic boundary slab containing a single layer of MoO_3. To study water adsorption on the lattice oxygens at different coverages and the influence of local chemical environment of the adsorption site on the adsorption properties, three kinds of models of the (010) surface with different sizes and shapes were adopted for the calculations of the adsorption systems.

Results and discussion

MoO_3 bulk

MoO_3 bulk with its layered structure is shown in Fig 1. First of all, the bulk comprising four MoO_3 units is optimized, relaxing both the lattice constants and atomic coordinates. The equilibrium structure obtained is illustrated in Fig 1, and the structural parameters of the lattice constants and bond lengths are tabulated in Tables 1 and 2, respectively. The calculated lattice constants are very close to the experimental values, [31] and deviations of *a*, *b* and *c* compared with experimental data [31] are 1.89%, 0.18% and 1.11%. Further, our calculated equilibrium bond lengths of various Mo–O bonds including van der Waals bonds of the Mo···O_1 shown in Table 2 are also in agreement with experimental values. [31] For example, the bond lengths of the Mo···O_1 are calculated to be 3.562 Å and 3.793 Å, in good agreement with experimental results of 3.526 Å and 3.794 Å. [31] All these agreements indicate that the methodologies used in the present study are effective for reproducing the MoO_3 crystal structure.

Our calculated band gap of bulk MoO_3 is 1.27 eV less than the experimental value of 3.66 eV, [32] and the binding energy obtained for the bulk is –2.798 Ry per unit cell. Thus, the small band gap is due to the DFT feature that often underestimates the band gap. A Mulliken population analysis gives results (see Table 3) consistent with previous studies. [5, 6] It is observed that the terminal oxygens are least ionic with charges of –0.430, which is very close to the value of –0.44 calculated by HF. [6] The doubly coordinated oxygens are ionic, while the triply coordinated become slightly more ionic. Charges on the lattice oxygen atoms decrease in the order: $q(O_3)>q(O_2)>q(O_1)$. Therefore, the highest coordinated oxygen atom bears the largest charge.

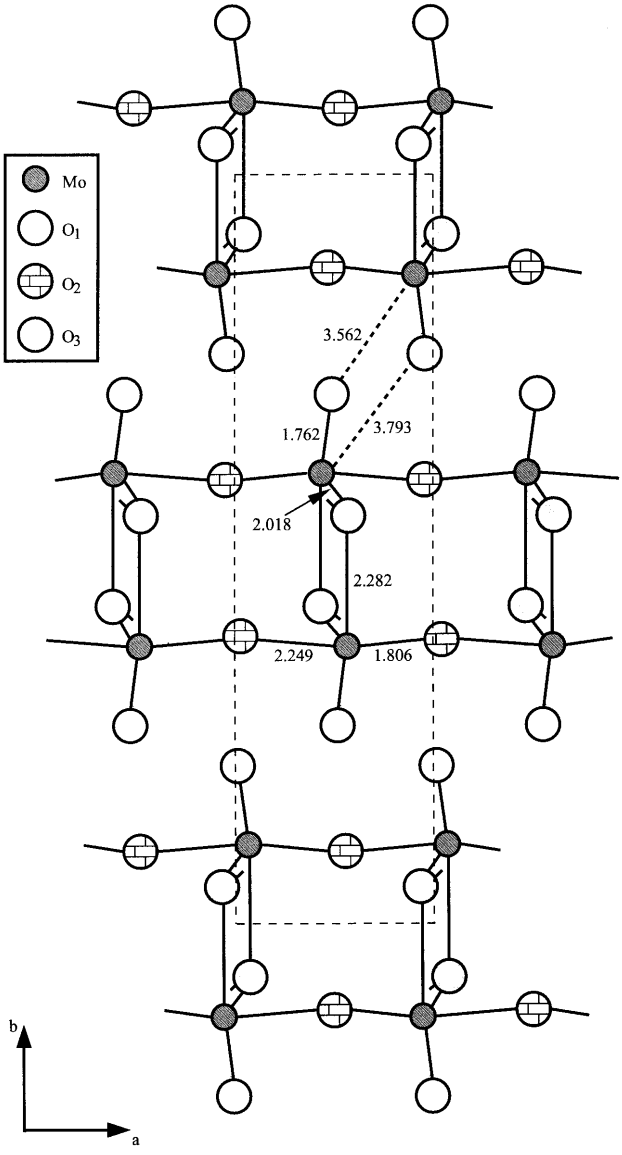

Fig. 1 Optimized Mo–O bond lengths (Å) in MoO_3 bulk. The broken lines indicate the unit cell projected onto the (*a*, *b*) plane

Table 1 Calculated lattice constants (Å) of MoO_3 bulk and (010) surface

Lattice constants		*a* (Å)	*b* (Å)	*c* (Å)
Calc.	Bulk	4.038	13.880	3.737
	Surface	4.039	–	3.738
Expt. [31]	Bulk	3.963	13.855	3.696

Table 2 Calculated bond lengths (Å) of Mo–O present in MoO_3 bulk and (010) surface

Bonds		Mo=O_1	Mo–O_2	Mo–O_2	Mo–O_3	Mo–O_3	Mo–O_3	Mo···O_1	Mo···O_1
Calc.	Bulk	1.762	1.806	2.249	2.018	2.018	2.282	3.562	3.793
	Surface	1.762	1.808	2.248	2.018	2.018	2.283	–	–
Expt. [31]	Bulk	1.678	1.683	2.303	2.025	2.025	2.312	3.526	3.794

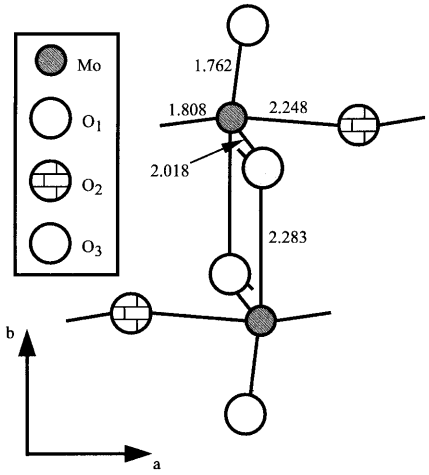

Fig. 2 Optimized Mo–O bond lengths (Å) in MoO_3(010) surface

Table 3 Mulliken charges of all the atoms in MoO_3 bulk and (010) surface

Atoms	Mo	O_1	O_2	O_3
Bulk	+1.857	–0.430	–0.712	–0.715
Surface	+1.764	–0.332	–0.720	–0.712

MoO_3 (010) surface

As described in the methods section, the interlayer interaction is so weak that MoO_3 cleaves easily along the (010) plane. Since only the weak bonds are broken, it is assumed that the remaining bonds are not modified such that the (010) surface essentially remains identical to a parallel bulk plane. [3] In this study, a clean MoO_3(010) surface was modeled as a slab composed of two MoO_3 units with a periodic boundary (see Fig 2), where full relaxations of the lattice constants (*a* and *c*) and atomic coordinates were carried out. Adjacent slabs were separated by a vacuum region with a thickness of more than 8 Å. At such a distance, interaction between the neighboring slabs is tiny.

The lattice constants of *a* and *c* were calculated to be 4.039 Å and 3.738 Å (see Table 1), almost identical to those of the bulk (the difference is only 0.001 Å). Again, all bond lengths of the Mo–O present in the (010) surface are extremely close to those in the bulk; the difference is at most 0.002 Å, as listed in Table 2. Essentially, charges on atoms on the MoO_3(010) surface are also very close to those of the bulk (Table 3). All these facts suggest that the MoO_3(010) surface and bulk have very similar geometric and electronic structures, consistent with the experimental finding. [3] The calculated charges show that the O_1 is the least ionic among all the surface oxygens, while the O_2 and O_3 atoms are more ionic than the O_1 and retain almost the same charges as in the case of the bulk. It is observed that charges on both the Mo and O_1 atoms in the (010) are considerably decreased by ca. 0.1 compared to those in the bulk, clearly indicating that the (010) surface is reduced due to the existence of only short Mo–O bonds on the surface. Since the longest Mo···O bonds that connect the neighboring MoO_3 layers are broken when the (010) surface is formed, charge redistribution takes place and this process leads to charge transfer mainly between the terminated O_1 and the Mo atoms. In contrast, the charge redistribution is very weak for the V_2O_5(010) surface, since the largest difference of atomic charges between V_2O_5 bulk and (010) surface is less than 0.04. [20]

The band gap of the (010) surface is calculated to be 1.27 eV, almost identical to that of the bulk (1.27 eV), and the binding energy is –2.794 Ry per cell consisting of four MoO_3 units, very close to the bulk value (–2.798 Ry). These results also support the above speculation of the similarity between the (010) surface and the bulk. As mentioned above, for both V_2O_5 and MoO_3 the (010) surfaces are the most exposed and the most stable, but they exhibit considerably different structural and chemical properties. Owing to the existence of the long V···O bond, V_2O_5 exposes several naked vanadiums that are chemically active as Lewis acid sites on the (010) surface. On the MoO_3(010) surface, however, there exist only short Mo–O bonds, indicating that the MoO_3 surface shows somewhat reduced activity relative to the V_2O_5(010). Probably this discrepancy gives rise to the difference in adsorption and catalytic properties.

Water adsorption on the (010) surface

H_2O adsorption on MoO_3(010) surface may be considered as a Lewis acid–base reaction. As a consequence, H atoms (Lewis acid) of the water molecule are able to interact with the surface oxygens (Lewis base). Thus, hydrogen bonding may be formed by the interaction between the H atoms and the surface oxygens. Although the water molecule has a large dipole moment and lone-pair electrons on its own oxygen, a coordination interaction hardly takes place on MoO_3(010) surface since there is no exposed Mo atom (Lewis acid site) on the stoichiometric surface. To investigate water adsorption on the lattice oxygens of the (010) surface at 1 and 0.5 monolayer coverages and the influence of the local environment of the adsorption site on adsorption states, we adopt the following models with different size and shape:

Model A: single supercell of the (010) surface composed of two MoO_3 units (refer to Fig 2)
Model B: doubling model A along the *a*-axis direction (four MoO_3 units, refer to Fig 3)
Model C: doubling model A along the *c*-axis direction (four MoO_3 units, refer to Fig 4)

Model A

When a water molecule approaches the O_1 site (i.e. coverage of H_2O on the surface is 1 monolayer), molecular

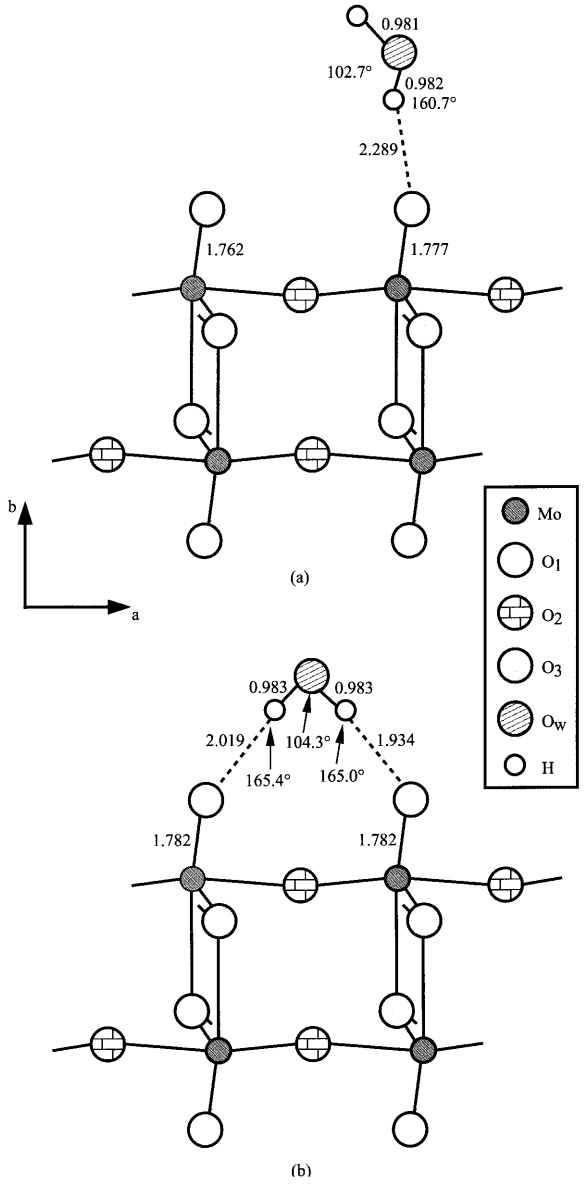

Fig. 3 Equilibrium interatomic distances (Å) and bond angles (deg) regarding the H_2O adsorption on the terminal oxygen(s) of MoO_3(010) surface of model B with the orientations of (a) on-top and (b) bridging. O_w designates the oxygen atom of the H_2O species

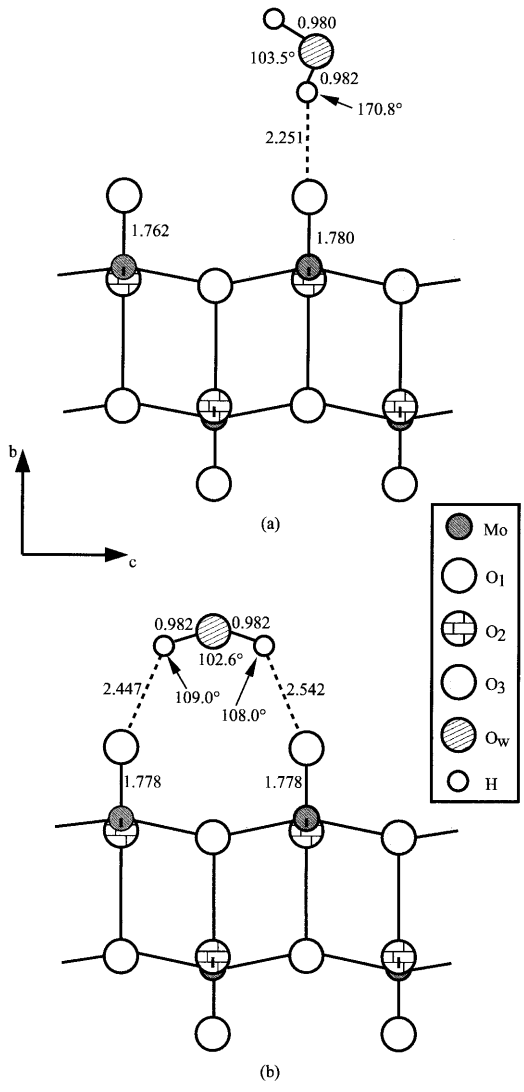

Fig. 4 Equilibrium interatomic distances (Å) and bond angles (deg) concerning the H_2O adsorption on the terminal oxygen(s) of MoO_3(010) surface of model C with the orientations of (a) on-top and (b) bridging. O_w denotes the oxygen atom of the H_2O species

adsorption takes place. The corresponding adsorption energy is calculated to be –6.83 kcal mol^{-1} (Table 4), indicating that the adsorption is energetically favorable and interaction between the adsorbate and substrate is rather strong. The equilibrium geometry obtained is shown in Fig 5, and the selected interatomic distances and bond angles are given in Table 5. The equilibrium geometry shows that the adsorption is caused by H-bonding between the H_2O species and the adsorption site (O_1). The $O_1\cdots$H–O bond has a length of 2.331 Å, and is nonlinear with a bond angle of 127.6°.

When going to the electronic properties (see Table 4), it is observed that charge on the O_1 site is nega-

Table 4 Mulliken atomic charges and adsorption energies with respect to the H_2O adsorption on the terminal oxygen of the MoO_3(010) surface

Orientations	Model A On-top	Model B		Model C	
		On-top	Bridging	On-top	Bridging
qH	+0.298	+0.285	+0.295	+0.289	+0.284
qH[a]	+0.259	+0.283	+0.295	+0.251	+0.285
qO	–0.526	–0.537	–0.446	–0.451	–0.493
$q(H_2O)$	+0.031	+0.031	+0.144	+0.089	+0.076
qO_1	–0.382	–0.440	–0.472	–0.446	–0.397
			–0.467		–0.391
ΔqO_1	–0.050	–0.108	–0.140	–0.114	–0.065
			–0.135		–0.059
ΔqMo(–O_1)	+0.018	+0.055	+0.049	+0.113	+0.089
			+0.038		+0.085
E_{ads} (kcal mol^{-1})	–6.83	–5.45	–3.44	–3.53	–5.52

[a] This contributes to H-bonding only for bridging adsorption

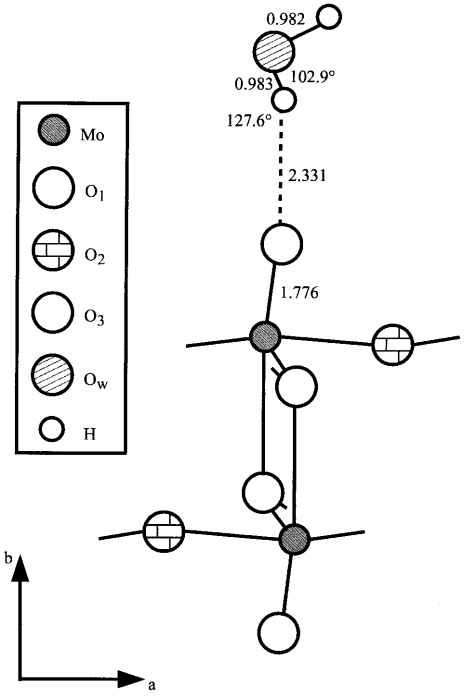

Fig. 5 Equilibrium interatomic distances (Å) and bond angles (deg) with respect to the H_2O adsorption on the terminal oxygen of MoO_3(010) surface of model A. O_w represents the oxygen atom of the H_2O species

Table 5 Selected interatomic distances (Å) and bond angles (degree) with respect to the H_2O adsorption on the terminal oxygen of the MoO_3(010) surface

Orientations	Model A On-top	Model B		Model C	
		On-top	Bridging	On-top	Bridging
*d*O–H (Å)	0.983	0.982	0.983	0.982	0.982
*d*O–H[a] (Å)	0.982	0.981	0.983	0.980	0.982
dO_1···H (Å)	2.331	2.289	2.019	2.251	2.447
			1.934		2.542
*d*Mo–O_1 (Å)	1.776	1.777	1.782	1.780	1.778
			1.782		1.778
∠H–O–H (deg)	102.9	102.7	104.3	103.5	102.6
∠O_1···H–O (deg)	127.6	160.7	165.4	170.8	109.0
			165.0		108.0

[a] This contributes to H-bonding only for bridging adsorption

tively increased by 0.050 compared with that of the stoichiometric surface, and the adsorbate species becomes positively charged. This means that the adsorbed water species donates 0.031 electrons to the surface, less than the increased charge on the O_1 site. This phenomenon clearly indicates that 0.019 electrons are donated to the O_1 site by other surface atoms. Our previous study [22] showed that the H-bond formed in a water dimer is nonlinear, and it is formed by electron donation from lone-pair electrons of the oxygen of one water molecule to the O–H antibonding orbital of another water molecule in the dimer. An increase in the negative charge on the O_1 site and corresponding increase in the positive charge on the H_2O species show that the nature of the H-bonding present in this system is different from that of the water dimer, which is very similar to the case of H_2O adsorption on V_2O_5(010). [22] As a matter of fact, there might be a donation of lone pair of electrons from the O_1 site to the water molecule, as in the case of the water dimer, but the net result shows that this donation is rather weak and it is dominated by the back-donation of the O–H bonding electrons from the water species to the O_1 site. At the same time, the positive charge on the molybdenum atom bound to the O_1 site is increased by 0.018, which is almost identical to the difference of the increased charges between the water species and the adsorption site O_1. The other molybdenum atoms on the surface essentially retain the same charges as on the clean surface. This suggests that there should be a charge flow from the Mo to the O site that happens only when there is a donation of electrons from the surface oxygen to the water species. All such processes result in the weakening of the O–H and Mo–O_1 bonds and they are elongated accordingly.

Model B

On-top adsorption. So far, the adsorption at 1 monolayer coverage has been investigated. To study the adsorption at 0.5 monolayer coverage and the effect of the local environment of the adsorption site on the adsorption, models B and C are used here. The distance between the two O_1 sites in model B is 4.039 Å, while that in model C is 3.738 Å. This difference may lead to different adsorption properties. Using the two models, adsorption states of H_2O with on-top and bridging orientations were examined.

When a water molecule is approaching the O_1 site, molecular adsorption takes place. The adsorption energy is calculated to be –5.45 kcal mol^{-1}, and the equilibrium geometry is illustrated in Fig 3a. The distance between the adsorption site and the H atom of the H_2O is found to be 2.289 Å, and the length of the Mo–O_1 bond is 1.777 Å, which is relaxed outward along the normal to the surface by 0.015 Å due to the adsorption (Table 5). The newly formed O_1···H–O bond is nonlinear with a bond angle of 160.7°. The other related structural parameters are also given in Table 5. Similar to the former case, the H_2O species takes the electronic charge of +0.031, indicating electron flow from the adsorbate to the substrate. The charge transferred from the adsorbate is accumulated at the adsorption site. Here also the increased charge on the adsorption site is much larger than that transferred from the adsorbate. It is observed that the Mo atom connected with the adsorption site increases its charge positively by 0.055, which demonstrates the electron flow from the Mo atom to the adsorption site. In addition, the ionicity of the O_1 and Mo in the O_1–Mo group and the H-bond angle here are larger than those in model A.

Bridging adsorption. When water molecule orients over the two O_1 sites of model B, molecular adsorption occurs. The adsorption energy is found to be –3.44 kcal mol^{-1}, which shows the possibility and stability of the adsorption. As shown in Fig 3b, two H-bonds are formed through the O_1 sites and two O–H bonds of the H_2O species. The two H-bonds are calculated to have slightly different lengths of 2.019 and 1.934 Å, respectively, and the Mo–O_1 bonds are elongated by 0.020 Å due to the interaction with the adsorbate. The bond angle ∠H–O–H in the adsorbed H_2O species is found to be 104.3°, larger than in the former two cases. The bond angles of the $\angle O_1 \cdots$H–O are calculated to be 165.4 and 165.0°, respectively. The two O–H bonds of the H_2O species are observed to be 0.983 Å, as shown in Fig 3b and Table 5.

When observing the electronic properties (Table 4), charges on the H atoms are both +0.295, while the charge on the O atom of the H_2O species is –0.446. This demonstrates that the H_2O species is polarized with a net charge of +0.144, which is similar to the former adsorption cases. This indicates that the H_2O species donates 0.144 electrons to the substrate. Each of the two adsorption sites of the O_1 atoms are observed to accumulate extra electrons of ca. 0.14, and the total charge increase on the two sites due to the adsorption is 0.275, larger than that donated from the H_2O species by 0.131. Two Mo atoms directly connected to the adsorption sites lose their charge totally by 0.087, which implies that 0.044 (0.131–0.087) electrons must be transferred from other surface atoms. This clearly shows that there must be an electron flow within the substrate plane, otherwise this phenomenon could not happen. This process may take place only when the electron donation from the sites to the water species becomes possible, as discussed above.

Model C

On-top adsorption. H_2O adsorption on top of the terminal oxygen O_1 of model C is also energetically possible, since the adsorption energy is –3.53 kcal mol^{-1}. However, this adsorption is less stable than the corresponding adsorption in models A and B. The optimized geometry and selected structural parameters are shown in Fig 4a and Table 5, respectively. It is observed that the adsorption site moves away from the substrate plane by 0.018 Å induced by the adsorption. The interacting distance between the H_2O species and the O_1 site is 2.251 Å, which is smaller than the on-top adsorption in models A and B. Similar to the former cases, the H_2O species is polarized and takes a positive charge of 0.089, while charge on the adsorption site is negatively increased by 0.114; accordingly the Mo atom bound to the adsorption site loses its electrons by 0.113. The newly formed H-bond of the $O_1 \cdots$H–O is nonlinear with a bond angle of 170.8°. It is found that the H-bond angle and ionicity of the adsorption site (O_1) and its closest Mo are larger than those in models A and B.

Bridging adsorption. The distance between the two O_1 sites of model C is 3.738 Å, smaller than that in model B. When two H atoms of a water molecule orient over the two O_1 sites, adsorption takes place and the adsorption energy is calculated to be –5.52 kcal mol^{-1}, larger than the bridging adsorption in model B. The equilibrated structure of the adsorption system is shown in Fig 4b. Due to the adsorption, two H-bonds are formed between the adsorption sites and the adsorbate species. The two H-bonds are 2.447 and 2.542 Å, respectively, much longer than the corresponding bond lengths found above. Correspondingly, the two Mo–O_1 bonds are elongated by 0.016 Å. The bond angles of the $\angle O_1 \cdots$H–O are found to be 109.0° and 108.0°, smaller than the corresponding bond angles found above by ca. 57°. This seems to be related to the short distance between the two O_1 sites. For the water species, the O–H bonds are 0.982 Å, and the angle of the ∠H–O–H is observed to be 102.6°, smaller than the corresponding angle in model B by 1.7°.

Similar to the adsorption in model B, the adsorbate and the substrate are polarized due to charge transfer. Again, it is observed that the adsorbed water donates 0.076 electrons to the surface, and the two adsorption sites accumulate 0.065 and 0.059 extra electrons, which is larger than the amount donated by the water species. This is caused mainly by the two Mo atoms closely connected to the adsorption sites, since they lose 0.089 and 0.085 electrons, respectively. This shows the redistribution of electrons on the (010) surface and the formation of H-bonds between the water species and the adsorption sites. The mechanism of forming the H-bonds here is also very similar to that in models A and B.

Discussion of the H_2O adsorption on the (010) surface

In order to evaluate the adsorption ability of the three distinct surface oxygens, a number of different initial orientations of the H_2O molecule on the surface have been taken into account, including on-top and bridging orientations over the O_2 and O_3 sites. With the geometry optimization involving the H_2O molecule and the adsorption site(s), it is observed that the water molecule shifts away from its initial position, and approaches the O_1. These phenomena clearly indicate that water adsorption on the MoO_3(010) surface prefers the O_1 site rather than the O_2 or O_3, which means that the terminal oxygen exhibits strong adsorption ability. This is probably due to the special local chemical environment of the O_2 and O_3 sites that are so close to the terminal oxygen, and to the H atom of the H_2O molecule, which interacts with the O_1 more strongly than with the O_2 or O_3, as clarified by H adsorption studies. [7, 9, 10, 11]

For the adsorption with the on-top mode on the terminal oxygen of models A, B and C, the adsorption energies increase in the order: A<B<C. Simultaneously, the ionicity of the adsorption site O_1 and its closest Mo atom, and the H-bond angles also demonstrate the same trend, but the H-bond lengths exhibit the opposite ordering. Concerning the bridging adsorption in models B and C, the adsorption energies decrease in the order: B>C. At the same time, the ionicity of the adsorption site O_1 and the H-bond angle show an identical order, while the H-bond lengths and ionicity of the Mo atom closely bound to the adsorption site show a completely different order. On the other hand, no matter whether the on-top or bridging adsorption modes is taken, it is always observed that the more the adsorption energy, the less the charge on the adsorption site O_1 (see Table 4). This correlation suggests that the less the charge on the O_1 site, the more the electron donation from the O_1 site to the H_2O species should be, indicating that the electron donation plays a crucial role in the H_2O adsorption on the MoO_3(010) surface.

As described above, the H-bonds are formed in all the cases treated in the current study. The bond lengths of the $O_1\cdots$H–O range from 1.934 to 2.542 Å, and they are nonlinear with bond angles between 108.0° and 170.8°. All angles of the ∠H–O–H of the adsorbate species in the adsorption systems are more or less decreased compared to the free water molecule due to the adsorption; this phenomenon is also found for the H_2O adsorption on V_2O_5(010) surface. [22] Through the present study, it is clearly observed that the nature of the H-bonding treated in this study is different from that of the water dimer. Here, there might be a donation of lone-pair electrons from the O_1 site to the water species, as in the case of the water dimer, but the net results show that this donation is so weak that it is dominated by the back-donation of the O–H bonding electrons from the water species to the adsorption site. Therefore, the H_2O species are positively charged and the substrate becomes polarized. Charge flow also takes place from the Mo atom closest to the adsorption site to the O_1 site. Such a redistribution of charges plays a very important role for adsorption systems, which has been confirmed by a number of studies. [22, 23, 33, 34, 35] All such processes result in the weakening of the O–H and Mo–O_1 bonds and accordingly they are elongated (see Table 5). However, the donation from the surface oxygen to the water molecule is less compared to the back-donation, as the surface oxygen O_1 is connected to the transition metal atom (Mo) and has less negative charge.

Conclusions

We have investigated structure and electronic properties of MoO_3 bulk and (010) surface as well as H_2O adsorption at 1 and 0.5 monolayer coverages on the surface using periodic boundary DFT calculations. Our calculated lattice constants of MoO_3 bulk are in good agreement with experimental results, and various bond lengths obtained for the Mo–O are also very close to experimental values. The terminal oxygen is found to be the least ionic among the three kinds of lattice oxygens. The bond lengths and atomic charges on the atoms of MoO_3(010) surface are calculated to be very close to those in the bulk. This study suggests that the structural and electronic properties of the (010) surface should be very similar to those of the bulk, in agreement with experimental findings.

In the present study it is found that the molecular adsorption hardly takes place on the asymmetric and symmetric oxygens, no matter whether the on-top or bridging modes are taken. The terminal oxygen is the only active site for water adsorption on the (010) surface. Energetically the most favored adsorption orientation for a water molecule on the surface is the on-top of the terminal oxygen at 1 monolayer coverage. The driving force of the molecular adsorption is observed to be hydrogen bonding formed between the adsorption site (i.e. the terminal oxygen) and the O–H group of the water species, and the donation of electrons from the surface oxygen site to the adsorbate is the dominant contributor. Due to the electron donation and back-donation between the water species and the (010) surface, both the adsorbate and the substrate become polarized.

References

1. Ono T, Nakajo T, Hironaka T (1990) J Chem Soc Faraday Trans 86:4077
2. Mestl G, Ruiz P, Delmon B, Knozinger H (1994) J Phys Chem 98:11269
3. Henrich VE, Cox PA (1996) The surface science of metal oxides. Cambridge University Press, Cambridge
4. Iizuka Y (1994) J Chem Soc Faraday Trans 90:1301
5. Papakondylis A, Sautet P (1996) J Phys Chem 100:10681
6. Cora F, Patel A, Harrison NM, Roetti C, Catlow CRA (1997) J Mater Chem 7:959
7. Hermann K, Michalak A, Witko M (1996) Catal Today 32:321
8. Michalak A, Hermann K, Witko M (1996) Surf Sci 366:323
9. Hermann K, Witko M, Michalak A (1997) Proceedings of Symposium on Advanced and Applications of Computational Chemical Modeling to Heterogeneous Catalysis, San Francisco, CA, p 106
10. Hermann K, Witko M, Michalak A (1999) Catal Today 50:567
11. Chen M, Waghmare UV, Friend CM, Kaxiras E (1998) J Chem Phys 109:6854
12. Chen M, Friend CM, Kaxiras E (2000) J Chem Phys 112:9617
13. Irigoyen B, Castellani N, Juan A (1998) J Mol Catal 129:297
14. Irigoyen B, Juan A, Castellani N (2000) J Catal 190:14
15. Tsipis AC (2000) Phys Chem Chem Phys 2:1357
16. Henrich VE (1985) Rep Prog Phys 48:1481
17. Smith MR, Ozkan US (1993) J Catal 142:226
18. (1997) CASTEP, MSI, San Diego
19. (1996) DSolid, MSI, San Diego
20. Yin X, Fahmi A, Endou A, Miura R, Gunji I, Yamauchi R, Kubo M, Chatterjee A, Miyamoto A (1998) Appl Surf Sci 130–132:539
21. Yin X, Han H, Endou A, Kubo M, Teraishi K, Chatterjee A, Miyamoto A (1999) J Phys Chem B 103:1263
22. Yin X, Fahmi A, Han H, Endou A, Ammal SSC, Kubo M, Teraishi K, Miyamoto A (1999) J Phys Chem B 103:3218

23. Yin X, Han H, Gunji I, Endou A, Ammal SSC, Kubo M, Miyamoto A (1999) J Phys Chem B 103:4701
24. Yin X, Han H, Miyamoto A (2000) Phys Chem Chem Phys 2:4243
25. Kohn W, Sham LJ (1965) Phys Rev A 140:1133
26. Perdew JP (1991) In: Ziesche P, Eschrig H (eds) Electronic Structure of Solids '91. Akademie Verlag, Berlin
27. Gordon MS, Binkley JS, Pople JA, Pietro WJ, Hehre WJ (1982) J Am Chem Soc 104:2797
28. Francl MM, Pietro WJ, Hehre WJ, Binkley JS, Gordon MS, Defrees DJ, Pople JA (1982) J Chem Phys 77:3654
29. Frisch MJ, Pople JA, Binkley JS (1984) J Chem Phys 80:3265
30. Braithwaite ER, Haber J (eds) (1994) Molybdenum: an outline of its chemistry and uses. Studies in inorganic chemistry, vol 19. Elsevier, Amsterdam
31. Kihlborg L (1963) Arkiv Kemi 21:357
32. Deb SK (1968) Proc R Soc London, Ser A 304:211
33. Nalewajski RF, Korchowiec J (1991) J Mol Catal 68:123
34. Nalewajski RF, Korchowiec J, Tokarz R, Broclawik E, Witko M (1992) J Mol Catal 77:165
35. Nalewajski RF, Koster AM, Bredow T, Jug K (1993) J Mol Catal 82:407